Ab Initio Investigation of CO Gas Sensing Mechanism on SnO_2 Surfaces

H.A. Zakaryan, V. M. Aroutiounian

Department of Physics of Semiconductors and Microelectronics
Yerevan State University
Yerevan, Republic of Armenia
email: zhayk91@gmail.com
email: aroutiounv1@yahoo.com

Abstract—This research is devoted to the investigation of the toxic CO gas adsorption mechanisms on the tin dioxide (SnO_2) semiconductor. We used density functional theory (DFT) to describe adsorption processes and found out that the Mars-van Krevelen (MvK) adsorption mechanism is not responsible for adsorption on (101) and (001) surface orientations of SnO_2, unlike for (110), (100), where CO_2 molecule forms and desorbs from the surfaces. Electronic density of states (eDoS) calculation and Bader charge analysis were done to explain the increase of surface conductance.

Keywords-gas; sensor; DFT; CO; adsorption; Mars-van Krevelen.

I. INTRODUCTION

Carbon monoxide (CO) is tasteless and transparent substance, which is known as an "invisible killer" due to the high level of toxicity. It is extremely poisonous and can even cause health effects up to a certain extent - 9ppm, therefore, the detection of CO in the environment is quite vital. For the above reasons, chemical sensors are used to precisely monitor the concentration of the target compounds in the air. Usually, the SnO_2 semiconductor is used as a sensing material in such detectors, because of high sensitivity and low response time for wide variety of molecules, such as CO, H_2, CH_3OH, NO_x, etc. [1]–[8]. In order to increase the sensitivity of the detectors, it is crucial to deeply investigate adsorption mechanism of CO compounds.

Several models, which are named as Langmuir Hishelwood [9][10], Eley Redeal [11] and the MvK [12], have been developed to describe the mechanisms that are responsible for CO adsorption on oxide semiconductors. The MvK adsorbtion mechanism is in a good agreement with the experiments on SnO_2–(110) surface [13][14]. Apparently, the MvK mechanism consists of following steps; *I)* adsorbed CO molecule is reacting with tin dioxide oxygen and forms CO_2 compound, leaving oxygen vacancy in the material; *II)* then remained vacancy fills by adsorbed O_2 molecule from the environment; *III)* and finally, another CO molecule is reacting with already bonded O_2 and

forms CO_2, leaving material in its initial undisturbed state.

We would like to stress that there are plenty of manuscripts dedicated to the investigation of CO absorption on SnO_2 surfaces, using first principle and ab initio DFT calculations [15][16]. Some calculations were done particularly for pristine (110) surface orientation [17], oxygen reach [18] and tainted surfaces [19]. However, very few are devoted to other surface orientations (100), (101) [5] and (001) [6]. In practice, surface orientation immensely influences sensor parameters such as sensitivity, time response etc.

In this manuscript, we explore CO adsorption on various surface orientations (110), (100), (101), (001) of SnO_2 and determine the most optimal configurations for adsorption, using ab initio DFT calculations in order to shed the light on the atomic scale processes that still remains elusive and unclear. Here, we will rise following issues: *I)* Does MvK mechanism similarly describing adsorption processes for all surface orientations of SnO_2? *II)* What is the exact amount of charge transferred between the surface and adsorbed CO molecule? *III)* Which surface orientation is more prominent to the interaction with the CO molecule?

The paper is organized in the following way: Section *II)* is devoted to computational methods and surface/bulk structure of SnO_2 sensing material. Section *III)* is devoted to the adsorption processes, eDoS calculations for the various surface orientations of SnO_2. Section *IV)* is dedicated to discussions and conclusions.

II. MODELS AND COMPUTATIONAL METHODS

Calculations were done using conventional ab initio DFT [20][21] method implemented in Vienna ab initio Simulation Package (VASP) [22]–[24]. DFT relaxations were done within Perdew-Burke-Ernzerhof (PBE) generalized gradient approximation (GGA) [25]. The 500eV cutoff energy was chosen due to the total energy convergence from that value. Surface structures were relaxed until the threshold net force on atoms become less than 0.01 eV/A. The Monkhorst-Pack scheme [26] was used to sample the Brillouin zone, using 6x6x1 k-points mesh. After relaxation, the
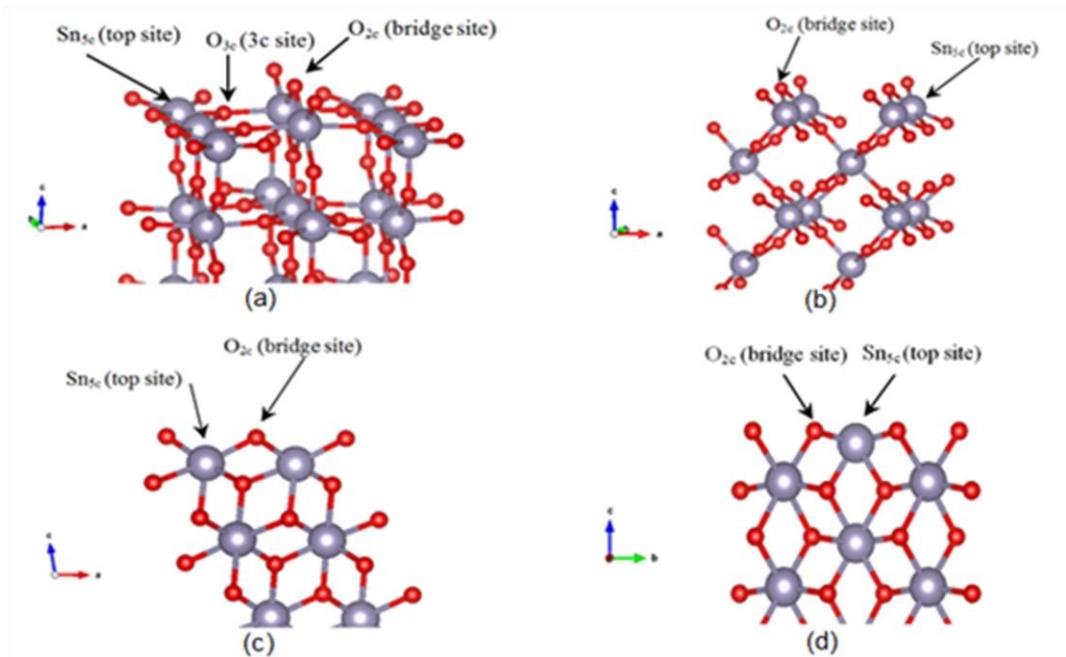
Figure 1. Different surfaces of SnO_2 and possible adsorption sites on it. a) (110) b) (100) c) (101) d) (001)

Bader charge analysis was done to find out charge transfer [27]–[29].

Stable adsorbed configurations were found using the following equation:

$$E_{ads}=E_{surf} - E_{clean} - E_{CO} , \qquad (1)$$

where E_{ads} is adsorption energy, E_{surf} is total energy of SnO_2 surface and adsorbed CO, E_{clean} is total energy of pure surface without CO and E_{CO} is total energy of the gas molecule. It is clear from this equation that if E_{ads} is negative the configuration of adsorbed site is stable, in other words, the process is exothermic. In the case of positive E_{ads}, the process is endothermic: the molecule will not adsorb to the surface and will remain in the non-interacting state.

Bulk SnO_2 has rutile, tetragonal structure, corresponding to the $P4_2/mnm$ space group. The lattice parameters of SnO2 from [30]–[32] are a = 4.82 Å, c = 3.23 Å and u = 0.607. In our calculations (see Fig. 1) each (110), (100), (101), (001) surface consists of 4 layers and relative stability has the following sequence (110), (100), (101), (001) [6]. Here, number of layers was tuned to check the convergence of surface energy. However, after getting all results, we double checked the obtained data by recalculating stable structures with a big substrate of 12 atoms of tin and 24 atoms of oxygen and make sure that the results are reliable. For all calculations, we choose vacuum thickness of 15 Å, which is greater than substrate thickness. For each surface, the electronic density of states (eDoS) was calculated and established that the gap between valence and conduction bands was underestimated,

because of the self-consistency of DFT calculations. From experiments, it is known that value of band gap is 3.6 eV, but we get 1 eV, which is in accordance with previous DFT calculations [33].

III. RESULTS AND DISCUSSION

In this section, each surface orientation would be described separately. Bader charge analysis, eDoS and stable structures would be presented as well.

A. SnO_2 (110) surface

This surface orientation consists of 4 layers, each comprising of 3 subsequent layers. Top sublayer represents oxygen, where each atom (O_{2c}) is connected by the covalent bond to 2 Sn atoms. The Second sublayer has 2 Sn atoms and 2 oxygen atoms. Third one is similar to the first layer. So, together these 3 sublayers can be treated as one layer which is continually repeated 4 times (see Fig1 a). There are 3 possible adsorption sites: top site (t), bridge site (br), three-coordinated oxygen site (3c). For each site, we consider 2 configurations: *I)* C atom in a CO molecule is closer to the surface (C down configuration) and *II)* the vice versa configuration (O down configuration). Thus, we end up with 6 possible configurations for (110) surface.

For each separate configuration calculated adsorption energies are given in Table I. As we can clearly see the O down configuration for all surfaces is completely unstable.

In the case of C down configuration, (110) surface has 3 stable sites. However, there is only one that is transferring the charge form molecule to the surface, and it is corresponding to the event when molecule approaches to br-site, reacts with oxygen and takes it away forming a CO_2 molecule and leaves oxygen vacancy on the surface. Here, vacancy could be an adsorption site for O_2 or CO molecule, as described in [15][18]. The eDoS of surface reveals that conductivity of the surface increases by decreasing of the band gap. The Bader charge analysis shows charge transport to the surface of 1.7e. Such processes examined in a number of experimental and theoretical studies [13][15][18]. It is important to note, that for this particular configuration and surface orientation the first step of MvK mechanism is preserved, and the distance between CO_2 molecule and surface is 3.1 Å.

For other sites (top and 3c) the CO molecule does not exchange electrons, which serves as a confirmation that we have physisorption process onto the surface. In these cases, band gap does not change and distances from carbon to tin atoms are 2.46, 2.61 Å, respectively.
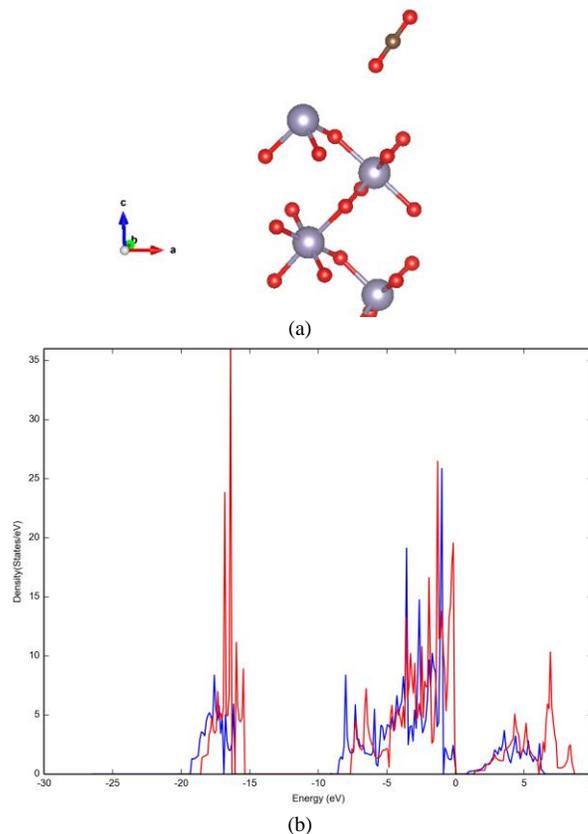

(a)

(b)

Figure 2. Structure and eDoS of (100) surface. a) Desorbed CO_2 molecule from (100) surface (red circle is oxygen, grey is Sn, brown is C atoms). b) eDoS of substrate before adsorption (red line), and after CO_2 desorption. (blue line).

TABLE I. ADSORPTION ENERGIES, DISTANCES AND BADER CHARGE ANALYSIS OF (110) SURFACE.

Ads. sites and configurations	Values of E_{ads}, distance and bader charge		
	$E_{ads}(eV)$	CO distanced surface(Å)	Charge transferred to surface(e)
br	-0.48	3.1	1.7
br(O down)	0.31	2.58	0.0
top	-0.16	2.465	0.0
top(O down)	0.01	2.69	0.0
3c	-0.03	2.61	0.0
3c(O down)	0.5	2.62	0.0

B. SnO$_2$ (100) surface

For (100) surface orientation the unit cell also consists of same 4 layers, where each layer can be divided into 3 sublayers: O-Sn-O layers. The top atom of the surface is 2 coordinated oxygen as in (110) surface, see Fig. 1 b. Adsorption energies for possible two site configurations are given in Table II. According to the calculations interaction of CO with the O_{2c} site of oxygen leads to the formation of CO_2 molecule and also leaves a vacancy on the surface (Fig. 2 a).

TABLE II. ADSORPTION ENERGIES, DISTANCES AND BADER CHARGE ANALYSIS OF (100) SURFACE.

Ads. sites	Values of E_{ads}, distance and bader charge		
	$E_{ads}(eV)$	CO distanced surface(Å)	Charge transferred to surface(e)
br	-0.48	3.25	1.6
top	-0.16	2.65	0.0

In this case, the first step of MvK mechanism is also conserved and it leads to charge transfer of 1.6e to the surface. Therefore, the surface conductance is increasing, because of transferred charge leading to the band gap reduction by 0.1eV in comparison to the uncharged surface, see Fig. 2 b. Here, the blue lines represent the eDoS after desorption that correspond to 3.25 Å distance from CO molecule to surface.

The Second possible adsorption site is top(t) on Sn atom. Here as for (110), the CO is physisorbed and no charge transfer has been observed. Due to physisorption, the distance from a carbon atom of CO molecule to the oxygen atom of the surface is 2.65 Å.

C. SnO₂ (101) surface

In the case of (101) surface orientation, each of 4 layers consists of 3 subsequent layers of 2O, 2Sn, 2O. There are 3 possible sites of adsorptions O_{2c}, Sn atom and 3 coordinated O, which is located in third sub layer as it is shown in Fig. 1 (c). Here, only one configuration has negative adsorption energy and it is O_{2c} (TABLE III).

TABLE III. ADSORPTION ENERGIES, DISTANCES AND BADER CHARGE ANALYSIS OF (101) SURFACE.

Ads. sites	Values of E_{ads}, distance and bader charge		
	$E_{ads}(eV)$	CO distanced surface(Å)	Charge transferred to surface(e)
O_{2c}	-0.47	1.18	1.9

The CO molecule adsorbs by the surface and remains connected to it in O_{2c} site with a distance of 1.18 Å (see Fig. 3). During that process, the distance between O_{2c} oxygen and Sn atom increases up to 2.5 Å. The Bader charge analysis shows that there is 1.9e charge transferred to the surface, which make it more conductive. Thus, adsorption mechanism on (101) surface differs from MvK, because no CO_2 desorption observed. Conductivity increases and band gap decreases due to transferred charge, see Fig. 3 (b), where blue lines represent eDoS after adsorption and have more states around Fermi level (Energy = 0 in the horizontal axis).

D. SnO₂ (001) surface

In this case, we have a completely different situation. Instead of 4 layers that consist of 3 subsequent layers, we have got only one that consists of one atom of Sn and 2 oxygen atoms. There are two possible sites: on top of Sn (t) site and O_{2c} (2c) site Fig. 1 (d). Moreover, there are 2 equivalent 2c sites in one unit cell, thus we should take into account two possible coverages. The first is when both sites are occupied by the CO molecule and form one mono layer (ML=1). The second possible coverage is when only one site is occupied and half mono layer of CO forms (ML = 0.5). For ML = 0.5, carbon monoxide adsorbed and stay bounded with a distance of 1.16 Å (Fig. 4) to the O_{2c} atom, transferring 2e charge to the substrate (see TABLE IV).

For ML = 1, one CO molecule adsorbed and one physisorbed in a 1.255 and 2.6 Å distances, respectively. In fact, for (001) only ML=0.5 coverage can happen, because when one CO adsorbed, the second one will be physisorbed. Bader charge analysis shows that 1.83e was transferred to the surface.
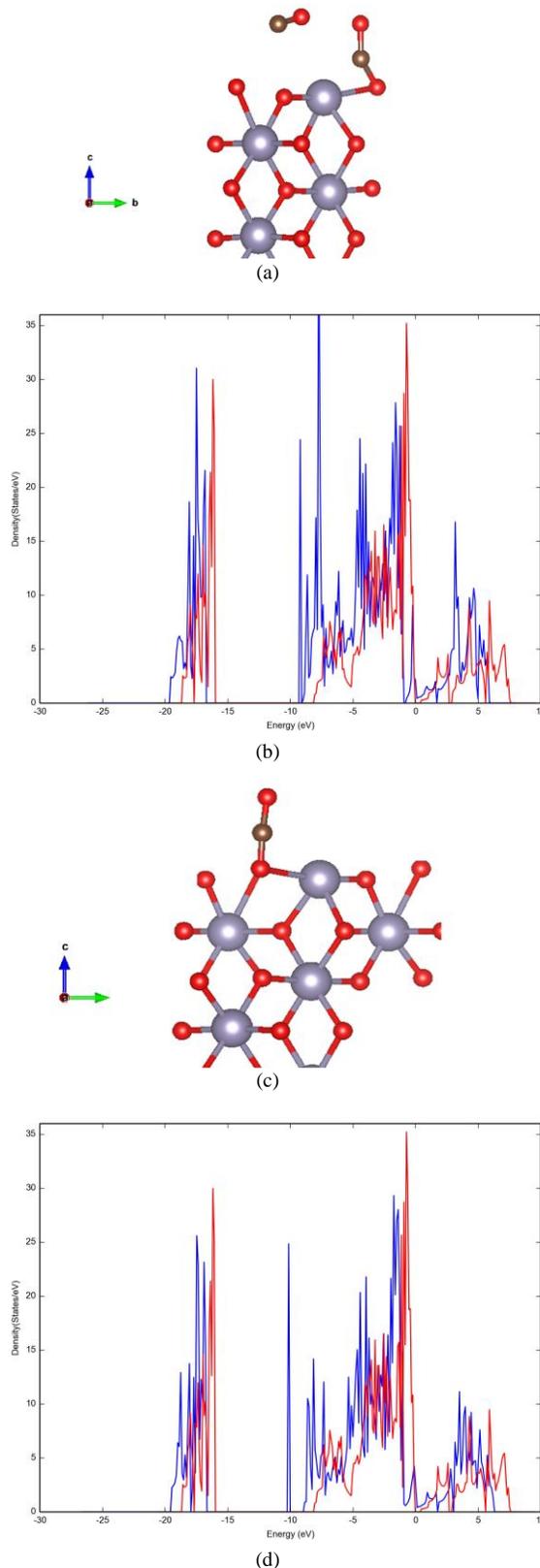

(a)

(b)

(c)

(d)

Figure 4. Configurations and eDoS of (001) surface (red circle is oxygen, grey is Sn, brown is C atoms). (a) Adsorption when ML=1.(b) eDoS before and after adsorption, when ML = 1 (b) Adsorption when ML= 0.5 (d)) eDoS before and after adsorption, when ML = 1.
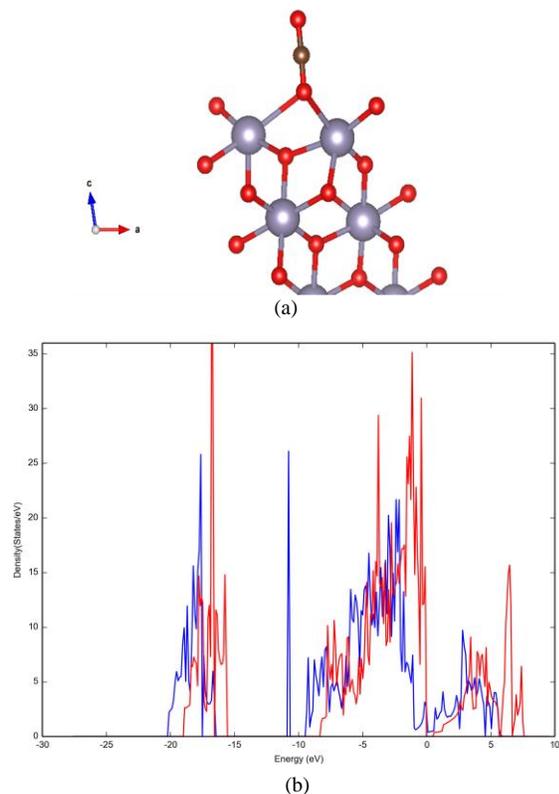
(a)

(b)

Figure 3.a) Adsorbed CO on (101) surface (red circle is oxygen, grey is Sn, brown is C atoms). b) eDoS of clean (101) surface (red line) and CO adsorbed on it (blue line).

TABLE IV. ADSORPTION ENERGIES, DISTANCES AND BADER CHARGE ANALYSIS OF (001) SURFACE.

Adsorption sites	Values of E_{ads}, distance and bader charge		
	$E_{ads}(eV)$	CO distanced surface(Å)	Charge transferred to surface(e)
2c, ML = 0.5	-1.19	1.16	2.0
2c, ML = 1	-1.24	1.25	1.8
top	-0.19	2.41	0.0

In both cases, surface conduction increases and band gap decreases due to charge transfer from the CO molecule. On Fig. 4 (b)(d), the red lines represent eDoS of undistorted surface and blue correspond to the eDoS after adsorption, which has more states around Fermi level compared to undistorted surfaces eDoS. Physisorption occurs for the top site with distance 2.41 Å.

IV. CONCLUSION

Previously, it was considered that adsorption on SnO_2 surfaces follows MvK mechanism; however, here we have proven that CO adsorption on SnO2(101), (001) is different. Here, the C atom of the CO molecule remains bonded to surface's O atom. Also, we find out that in the case of (001) surface

orientation CO coverage can be only half mono layer (ML = 0.5). For (110) and (100) surfaces, we establish that adsorption obeys MvK mechanism, where its first stage CO_2 molecules are forming during CO-surface interaction. For all adsorption cases, O down configuration was not stable, due to positive adsorption energy.

The Bader charge analysis reveals that charge transfer to (101), (001) surfaces are 1.9e, 2e respectively and 1.7e, 1.6e for (110), (100) surfaces. The eDoS combined with Bader analysis shows that (101), (001) surface orientations gather more electrons than the rest orientations, thus, those should be considered as a better platform for the interaction of the CO molecules with SnO2 surfaces. We believe that our findings will pave the way for the fabrication of SnO2 based CO sensors with higher sensitivity and lower response time.

REFERENCES

[1] V. Aroutiounian, "Metal oxide hydrogen, oxygen, and carbon monoxide sensors for hydrogen setups and cells," Int. J. Hydrog. Energy, vol. 32, no. 9, Jun. 2007, pp. 1145–1158, doi:10.1016/j.ijhydene.2007.01.004.

[2] V. M. Aroutiounian, "Metal oxide gas sensors decorated with carbon nanotubes," Lith. J. Phys., vol. 55, no. 4, Dec. 2015, pp. 319–329, doi:10.3952/physics.v55i4.3230.

[3] V. M. Aroutiounian et al., "Manufacturing and investigations of i-butane sensor made of SnO2/multiwall-carbon-nanotube nanocomposite," Sens. Actuators B Chem., vol. 173, Oct. 2012, pp. 890–896, doi:10.1016/j.snb.2012.04.039.

[4] M. Batzill and U. Diebold, "The surface and materials science of tin oxide," Prog. Surf. Sci., vol. 79, no. 2–4, 2005, pp. 47–154, doi:10.1016/j.progsurf.2005.09.002.

[5] S. Gong et al., "Gas sensing characteristics of SnO2 thin films and analyses of sensor response by the gas diffusion theory," Mater. Sci. Eng. B, vol. 164, no. 2, Aug. 2009, pp. 85–90, doi:10.1016/j.mseb.2009.07.008.

[6] C. Xu, Y. Jiang, D. Yi, S. Sun, and Z. Yu, "Environment-dependent surface structures and stabilities of SnO2 from the first principles," J. Appl. Phys., vol. 111, no. 6, Feb. 2012, pp. 63504 1-9, doi:10.1063/1.3694033.

[7] A. Adamyan et.al, "Sol–gel derived thin-film semiconductor hydrogen gas sensor," Int. J. Hydrog. Energy, vol. 32, no. 16, Nov. 2007, pp. 4101–4108, doi:10.1016/j.ijhydene.2007.03.043.

[8] A. Z. Adamyan, Z. N. Adamyan, and V. M. Aroutiounian, "Study of sensitivity and response kinetics changes for SnO2 thin-film hydrogen sensors," Int. J. Hydrog. Energy, vol. 34,

no. 19, Oct. 2009, pp. 8438–8443, doi:10.1016/j.ijhydene.2009.08.001.

[9] R. H. Nibbelke, M. A. J. Campman, J. H. B. J. Hoebink, and G. B. Marin, "Kinetic Study of the CO Oxidation over Pt/γ-Al2O3and Pt/Rh/CeO2/γ-Al2O3in the Presence of H2O and CO2," J. Catal., vol. 171, no. 2, Oct. 1997, pp. 358–373, doi:10.1006/jcat.1997.1785.

[10] I. Langmuir, "The mechanism of the catalytic action of platinum in the reactions 2Co + O2= 2Co2 and 2H2+ O2= 2H2O," Trans. Faraday Soc., vol. 17, 1922, pp. 621–654, doi:10.1039/tf9221700621.

[11] C. C. Cheng, S. R. Lucas, H. Gutleben, W. J. Choyke, and J. T. Yates, "Atomic hydrogen-driven halogen extraction from silicon(100): Eley-Rideal surface kinetics," J. Am. Chem. Soc., vol. 114, no. 4, Feb. 1992, pp. 1249–1252, doi:10.1021/ja00030a020.

[12] P. Mars and D. W. van Krevelen, "Oxidations carried out by means of vanadium oxide catalysts," Chem. Eng. Sci., vol. 3, 1954, pp. 41–59, doi:10.1016/S0009-2509(54)80005-4.

[13] Y. Sun et.al, "Atomically Thin Tin Dioxide Sheets for Efficient Catalytic Oxidation of Carbon Monoxide," Angew. Chem. Int. Ed., vol. 52, no. 40, Sep. 2013, pp. 10569–10572, doi:10.1002/anie.201305530.

[14] J. Yu, D. Zhao, X. Xu, X. Wang, and N. Zhang, "Study on RuO2/SnO2: Novel and Active Catalysts for CO and CH4 Oxidation," ChemCatChem, vol. 4, no. 8, Aug. 2012, pp. 1122–1132, doi:10.1002/cctc.201200038.

[15] Z. Lu et al., "Direct CO oxidation by lattice oxygen on the SnO 2(110) surface: a DFT study," Phys Chem Chem Phys, vol. 16, no. 24, 2014, pp. 12488–12494, doi:10.1039/C4CP00540F.

[16] M. Melle-Franco and G. Pacchioni, "CO adsorption on SnO2(110): cluster and periodic ab initio calculations," Surf. Sci., vol. 461, no. 1–3, Aug. 2000, pp. 54–66, doi:10.1016/S0039-6028(00)00528-8.

[17] F. Ciriaco, L. Cassidei, M. Cacciatore, and G. Petrella, "First principle study of processes modifying the conductivity of substoichiometric SnO2 based materials upon adsorption of CO from atmosphere," Chem. Phys., vol. 303, no. 1–2, Aug. 2004, pp. 55–61, doi: 10.1016/j.chemphys.2004.05.005.

[18] X. Wang, H. Qin, Y. Chen, and J. Hu, "Sensing Mechanism of SnO2 (110) Surface to CO: Density Functional Theory Calculations," J. Phys. Chem. C, vol. 118, no. 49, Dec. 2014, pp. 28548–28561, doi:10.1021/jp501880r.

[19] Y. B. Xue and Z. A. Tang, "Density functional study of the interaction of CO with undoped and Pd doped SnO2(110) surface," Sens. Actuators B Chem., vol. 138, no. 1, Apr. 2009 pp. 108–112, doi:10.1016/j.snb.2009.02.030.

[20] P. Hohenberg and W. Kohn, "Inhomogeneous Electron Gas," Phys. Rev., vol. 136, no. 3B, Nov. 1964, pp. B864–B871, doi:10.1103/PhysRev.136.B864.

[21] W. Kohn and L. J. Sham, "Self-Consistent Equations Including Exchange and Correlation Effects," Phys. Rev., vol. 140, no. 4A, Nov. 1965, pp. A1133–A1138, doi:10.1103/PhysRev.140.A1133.

[22] G. Kresse and J. Hafner, "Ab initio molecular dynamics for liquid metals," Phys. Rev. B, vol. 47, no. 1, Jan. 1993, pp. 558–561, doi:10.1103/PhysRevB.47.558.

[23] G. Kresse and J. Hafner, "Ab initio molecular-dynamics simulation of the liquid-metal–amorphous-semiconductor transition in germanium," Phys. Rev. B, vol. 49, no. 20, May 1994, pp. 14251–14269, doi:10.1103/PhysRevB.49.14251.

[24] G. Kresse and J. Furthmüller, "Efficient iterative schemes for ab initio total-energy calculations using a plane-wave basis set," Phys. Rev. B, vol. 54, no. 16, Oct. 1996, pp. 11169–11186, doi:10.1103/PhysRevB.54.11169.

[25] J. P. Perdew, K. Burke, and M. Ernzerhof, "Generalized Gradient Approximation Made Simple," Phys. Rev. Lett., vol. 77, no. 18, Oct. 1996, pp. 3865–3868, doi:10.1103/PhysRevLett.77.3865.

[26] H. J. Monkhorst and J. D. Pack, "Special points for Brillouin-zone integrations," Phys. Rev. B, vol. 13, no. 12, Jun. 1976, pp. 5188–5192, doi:10.1103/PhysRevB.13.5188.

[27] G. Henkelman, A. Arnaldsson, and H. Jónsson, "A fast and robust algorithm for Bader decomposition of charge density," Comput. Mater. Sci., vol. 36, no. 3, Jun. 2006, pp. 354–360, doi:10.1016/j.commatsci.2005.04.010.

[28] E. Sanville, S. D. Kenny, R. Smith, and G. Henkelman, "Improved grid-based algorithm for Bader charge allocation," J. Comput. Chem., vol. 28, no. 5, Apr. 2007, pp. 899–908, doi:10.1002/jcc.20575.

[29] W. Tang, E. Sanville, and G. Henkelman, "A grid-based Bader analysis algorithm without lattice bias," J. Phys. Condens. Matter, vol. 21, no. 8, Feb. 2009, pp.84204 1-7, doi:10.1088/0953-8984/21/8/084204.

[30] T. T. Rantala, T. S. Rantala, and V. Lantto, "Surface relaxation of the (110) face of rutile SnO2," Surf. Sci., vol. 420, no. 1, Jan. 1999, pp. 103–109, doi:10.1016/S0039-6028(98)00833-4.

[31] I. Manassidis and M. j. Gillan, "First-principles study of SnO2 (110)," Surf. Rev. Lett., vol. 1, no. 4, Dec. 1994, pp. 491–494, doi10.1142/S0218625X94000503.

[32] T. T. Rantala, T. S. Rantala, and V. Lantto, "Electronic structure of SnO2 (110) surface," Mater. Sci. Semicond. Process., vol. 3, no. 1–2, Mar. 2000, pp. 103–107, doi:10.1016/S1369-8001(00)00021-4.

[33] Y. Duan, "Electronic properties and stabilities of bulk and low-index surfaces of SnO in comparison with Sn O 2 : A first-principles density functional approach with an empirical correction of van der Waals interactions," Phys. Rev. B, vol. 77, no. 4, Jan. 2008, pp. 045332 1-22 doi:10.1103/PhysRevB.77.045332.